UNIVERSITÀ DEGLI STUDI DI PADOVA

Dipartimento di Fisica e Astronomia "Galileo Galilei"

Bachelor Degree in Physics

Final Dissertation

Study of the energy calibration of the mini-JUNO setup
Studio della calibrazione in energia del setup sperimentale mini-JUNO

Thesis supervisor
Alberto Garfagnini
Thesis co-supervisor
Arsenii Gavrikov

Candidate
Davide Marchesini

Academic Year 2022/2023

Contents

1 Abstract

The Jiangmen Underground Neutrino Observatory (JUNO) is a large liquid scintillator neutrino detector under construction in South Cina. The main goal of the experiment is to measure the neutrino oscillation parameters with sub-percent precision and to determine the neutrino mass ordering at 3-4 σ significance level after 6 years of data taking. The core of the experiment is a 35.4 m diameter spherical vessel filled with high purity, large mass (20 kton) liquid scintillator target. The acrylic vessel is surounded by 17612 20-inch and by 25600 3-inch photomultipliers, respectively. To achieve the physics goals, several challenges have been set, one of those is a requirement of a very good energy resolution of at least 3% at 1 MeV. To study the detector electronics response, a mini-JUNO setup with 20 liters of JUNO liquid scintillator, seen by 48 2-inch photomultipliers read by the final JUNO readout electronics, has been build at the Legnaro INFN laboratories. The purpose of the thesis is to study the energy response of the setup to cosmic muons and to calibration gamma sources.

Il Jiangmen Underground Neutrino Observatory (JUNO) è un grande rivelatore di neutrini a scintillatore liquido attualmente in costruzione nella Cina meridionale. L'obiettivo principale dell'esperimento è misurare i parametri dell'oscillazione dei neutrini con precisione inferiore al punto percentuale e determinare l'ordine di massa dei neutrini con un livello di significatività di 3-4 σ dopo 6 anni di acquisizione dati. Il nucleo dell'esperimento è una sfera di 35.4 m di diametro riempita con un bersaglio di scintillatore liquido ad alta purezza e grande massa (20 kton). La sfera di acrilico è circondata rispettivamente da 17612 fotomoltiplicatori da 20 pollici e da 25600 fotomoltiplicatori da 3 pollici. Per raggiungere gli obiettivi di fisica, sono state poste diverse sfide, tra cui il requisito di una risoluzione energetica molto elevata di almeno 3% a 1 MeV. Per studiare la risposta elettronica del rivelatore, è stato realizzato un sistema di mini-JUNO con 20 litri di scintillatore liquido JUNO, osservato da 48 fotomoltiplicatori da 2 pollici connessi all'elettronica finale di lettura di JUNO, presso i laboratori dell'INFN di Legnaro. Lo scopo della tesi è studiare la risposta energetica del sistema ai muoni cosmici e alle sorgenti di calibrazione gamma.

2 Introduction

The Jiangmen Underground Neutrino Observatory (JUNO) [1] is a neutrino scintillator detector under construction in South China, expected to start detector commisioning in 2024. The main goal of the experiment is to measure the neutrino mass ordering (NMO) at $3-4\sigma$ significance level and to measure the neutrino oscillation parameters with sub-percent precision [2]. JUNO will measure the energy spectrum of neutrinos as shown in figure 1.

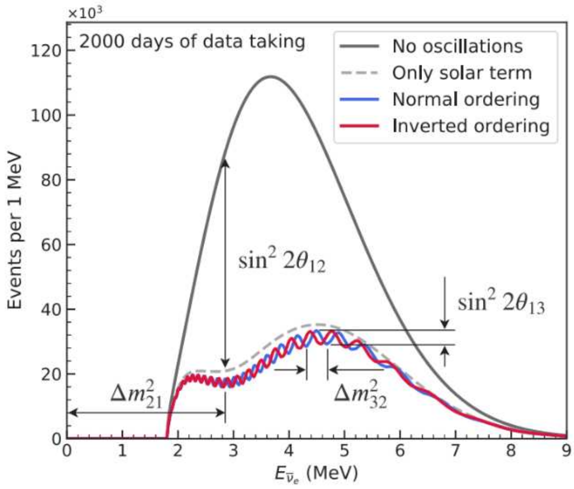

Figure 1: Expected energy distribution in JUNO (taken from [2])

The blue line is referred to Normal Ordering (NO) while the red line to the Inverted Ordering (IO). Moreover, by measuring the energy spectrum it will be possible to extrapolate the neutrino oscillation parameters with high precision [2].

Moreover, JUNO will be able to measure neutrino burst of supernova, solar neutrinos, geological neutrinos and neutrinos coming from other sources. The location of the experiment has been chosen near the Yangjiang and Taishan's Taishan Nuclear Power Plants; reactor antineutrinos are the primary neutrinos source in the JUNO detector.

Figure 2: Location of JUNO

The physical process that allows to observe the antineutrinos is the inverse β decay $\bar{\nu}_e + p \rightarrow n + e^+$ where the proton is given by the organic liquid scintillator. The final state positron annihilates with an electron producing two photons of $2 \cdot 511\text{keV}+T_{e^+}$, where the last term is the kinetic energy of the positron, which is of similar value of the antineutrino's energy. The neutron is captured on protons, and after approximately 200μs, a 2.2MeV photon is emitted providing a delayed signal as signature of the IBD interaction process.

The JUNO detector consists of a Central Detector (CD), a Water Cherenkov detector and a Top Tracker (TT). A schematic view of the JUNO detector is shown in the figure 3. The CD is filled with liquid scintilator (LS) with a designed effective energy resolution of $\sigma_E/E = \frac{3\%}{\sqrt{E(MeV)}}$ and mass around 20kton. The LS is contained in a spherical acrylic vessel, the PhotoMultiplier Tubes (PMTs) are inserted in the inner surface and all the vessel is submerged in a water pool (Cherenkov detector) equipped with PMTs. The PMTs are divided in two types: 17612 "Large PMTs" with 20-inch diameter and 25600 "Small PMTs" with 3-inch diameter.

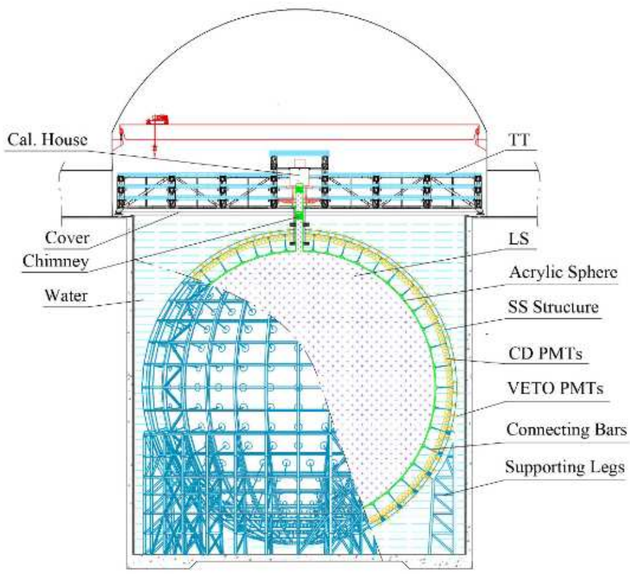

Figure 3: Lateral section of the JUNO detector (taken from [1])

The JUNO readout electronics is designated to achieve a maximum resolution in the data of the MeV order. To do so the PMTs must have a high photon efficiency, a stable operation system, a high reliability of the product (it is impossible to replace a single PMT over the years and it is required a loss of less than 0.5% in 6 years), and most importantly a low background noise (called dark noise). A scheme of the readout electronic is given in figure 4.

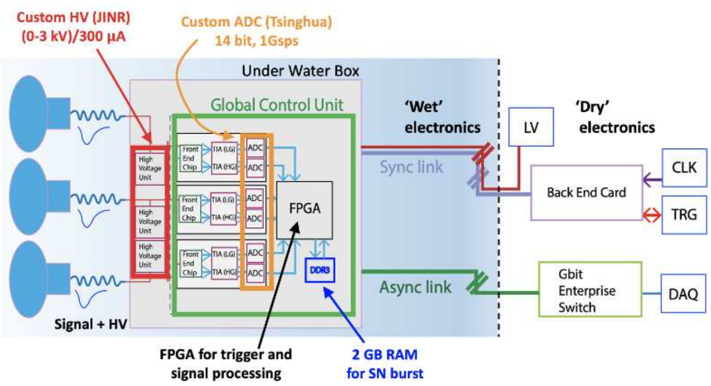

Figure 4: Scheme of the large PMT readout electronic (taken from [1])

The electronics chain is composed of two parts [3]: the front-end (FE), or wet electronics, located very close to the PMT output, inside the JUNO Water Pool; and the dry electronics, installed in the electronics room of the JUNO underground laboratories, and consisting of the back-end (BE) electronics and the data acquisition (DAQ) system.

Three PMT output signals are fed to one Under Water Box (UWbox) which contains three High Voltage Units (HVU) and a Global Control Unit (GCU). The PMT analog signal reaching the GCU is processed by a custom Front-End Chip (FEC), which splits the input signal and amplifies it with two different gains. The PMTs are connected to the UWbox electronics with a 50Ω. The electronics inside the UWbox has two independent connections to the BE electronics: a so-called synchronous link (S-link), which provides the clock and synchronization to the boards and handles the trigger primitives, and an asynchronous link (A-link) which is fully dedicated to the DAQ and slow-control, or Detector Control System (DCS).

3 The JUNO Legnaro setup

At the Laboratori Nazionali di Legnaro (LNL), in Italy, a mini-JUNO setup has been constructed to test and validate the large PMT readout electronic [3][4]. The experiment is a mock-up system of the one present in China but reduced in components, for example there is no Water Cherenkov detector and one of the important difference is that the "wet electronic" is not underwater, reducing all the related problems.

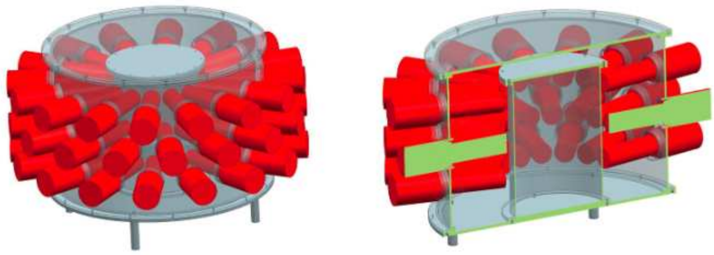

Figure 5: Technical drawing of the mini-JUNO setup (taken from [4])

The setup is composed of:

- an inner plexiglas cylindrical vessel which contains 17 litres of liquid scintillator LAB as solvent, doped with Poly-Phenylene Oxide (PPO) and bisMSB, with the same mixture of JUNO;
- the vessel is surrounded, only on the lateral surface, by 48 Philips XP2020 PMTs of circa 5cm radius controlled by 16 GCU divided in 3 different levels;
- the LS vessel and all the PMTs are surrounded by black plastic cylinder to shield from external light interference;
- finally, three plastic scintillators are used for the cosmic muon trigger, one at the top of the LS vessel and two at the bottom.

The PMTs characteristics are the followings: they have a low noise background, around 900counts/s (as it will be calculated in the data analysis), a good linear response (which is the topic of this thesis) and a good time response, fundamental for the characterization of correlated time waveform signals.

The data file for each run is converted from raw data to a ROOT file [5], in which a TTree object is written containing information in each TBranch. There are present and will be used later on this thesis:

- the active channels, the PMTs who are recording a signal
- the complete signal waveform, as shown in figure 6, in which three zones are visible : the first 60 points which help measure the baseline and define the trigger, the integration window in which there is the decay of the signal, residuals points to consider all the waveform and to not lose any signal
- some calculated information like the total charge, the multiplicity (the number of PMTs per event that receive a physical signal defined by the trigger threshold), the minimum of the waveform, the baseline (calculated as the average of the first 60 points) and the standard deviation of the baseline

- the event timestamp, the trigger begin time (time at which the signal surpass the trigger threshold) and the trigger end time.

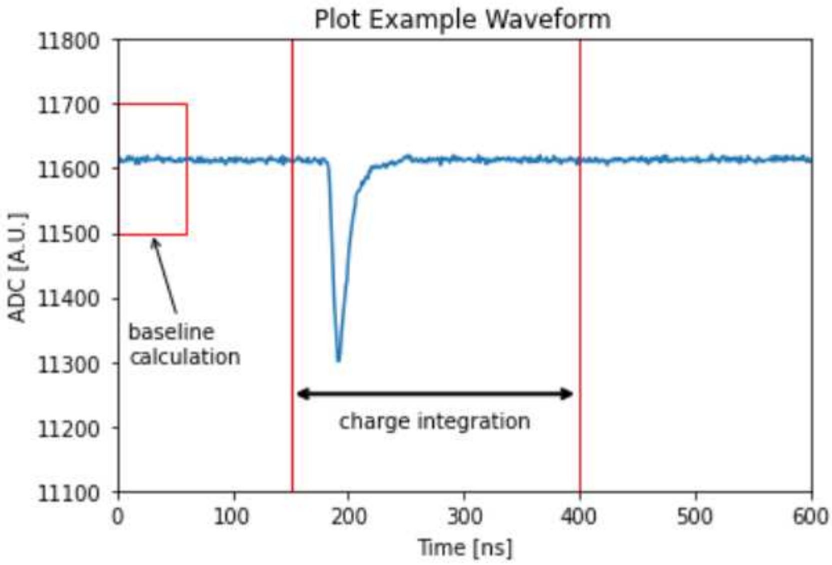

Figure 6: Example of waveform produced by one single PMT, emphasizing the baseline calculation window and the charge integration range

4 Energy calibration Runs

4.1 Runs acquisition

The main work of this thesis is the energy calibration of the Legnaro mini-JUNO setup. Using the PMTs of the setup, the total collected charge has been reconstructed and its response has been studied using few external gamma calibration sources and cosmic muons going through the detector. Due to the limited size of the liquid scintillator vessel, the full energy peak due to the energy deposit of the gamma sources is not visible: most of the photons perform one or two Compton interactions in the scintillator, before exiting the target vessel. Therefore, the calibration will use the Compton Edge of the energy release in the liquid scintillator [4].

The following calibration sources have been used [6]:

- ^{22}Na which decays, via β^+ with 99.9% probability, to an excited state of ^{22}Ne. The latter emits a 1275keV photon which may interact in the liquid scintillator.
- ^{60}Co decaying β^- to ^{60}Ni excited state. The latter decays to the fundamental states emitting two photons of 1173keV and 1332keV energy, in sequence.

Moreover, cosmic muons traversing vertically the liquid scintillator vessel are analyzed.

The radioactive sources have been positioned on the top of the setup and collimated using a lead brick in order to produce a photon beam impinging vertically on the liquid scintillator.

Four data acquisition runs have been collected:

- one cosmic muons run;
- one background run, without calibration sources;
- one ^{60}Co run;
- one ^{22}Na run.

The following configuration parameters have been used for the runs:

- the cosmic muon run has been collected using an external trigger, while the other runs have been collected by selecting a multiplicity trigger of at least 5 PMTs providing a signal in coincidence inside a 8 ns trigger window;
- the threshold for generating a local trigger on the readout board has been set at five times the baseline standard deviation;
- the cosmic muons trigger is generated by the coincidence of three plastic scintillators located above and below the liquid scintillator vessel;
- the cosmic muon run was taken over 60 minutes, while the other three runs (background and gamma source runs) over 15 minutes;
- for the computation of the integrated charge, the signal, baseline subtracted, has been integrated over a fixed time window. Since all the collected waveforms have a fixed and well defined pre-trigger, the integration windows is defined between 150 ns and 400 ns (see figure 6)

4.2 Data control

Before performing the analysis with the files it is necessary to execute a preliminary data control and data quality checks. Table 1 reports, for each run, the total number of acquired events and the number of events surviving all the analysis cuts.

Source	Number of events	Number of events after data control
^{60}Co	1288488	898106
^{22}Na	708970	418224
background	599934	348380
muons	8644	3387

Table 1: Number of events analyzed

The following cuts have been applied:

- even though mini-JUNO has 48 total channels, not all of them were fully working during the acquisition runs. The plots of figure 7 show the distribution of the number of active channels for the four runs. The cut $N_{active} \geq 45$ has been applied to all runs.

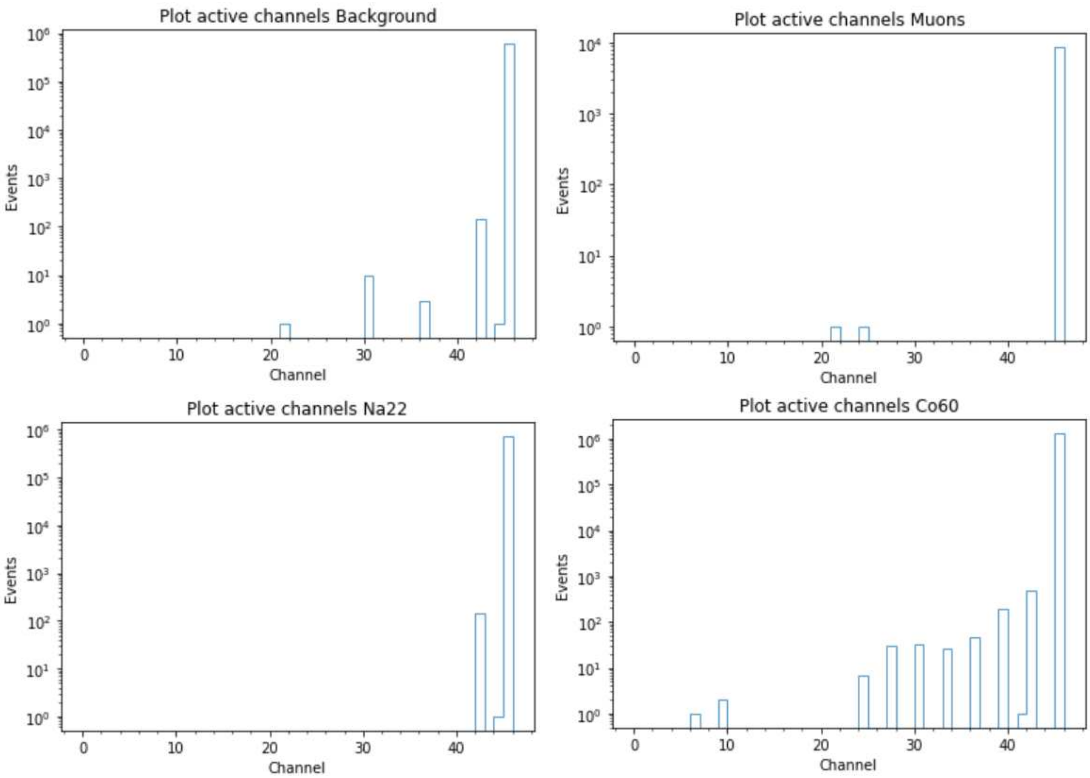

Figure 7: Histogram of the events for number of active channel of the four runs

- the background and gamma sources runs have been collected requiring a multiplicity of at least 5 PMTs for each event. The plot of figure 8 shows the multiplicity distribution for the four runs. A cut of $N_{PMT} \geq 5$ has been applied to the background and gamma runs.

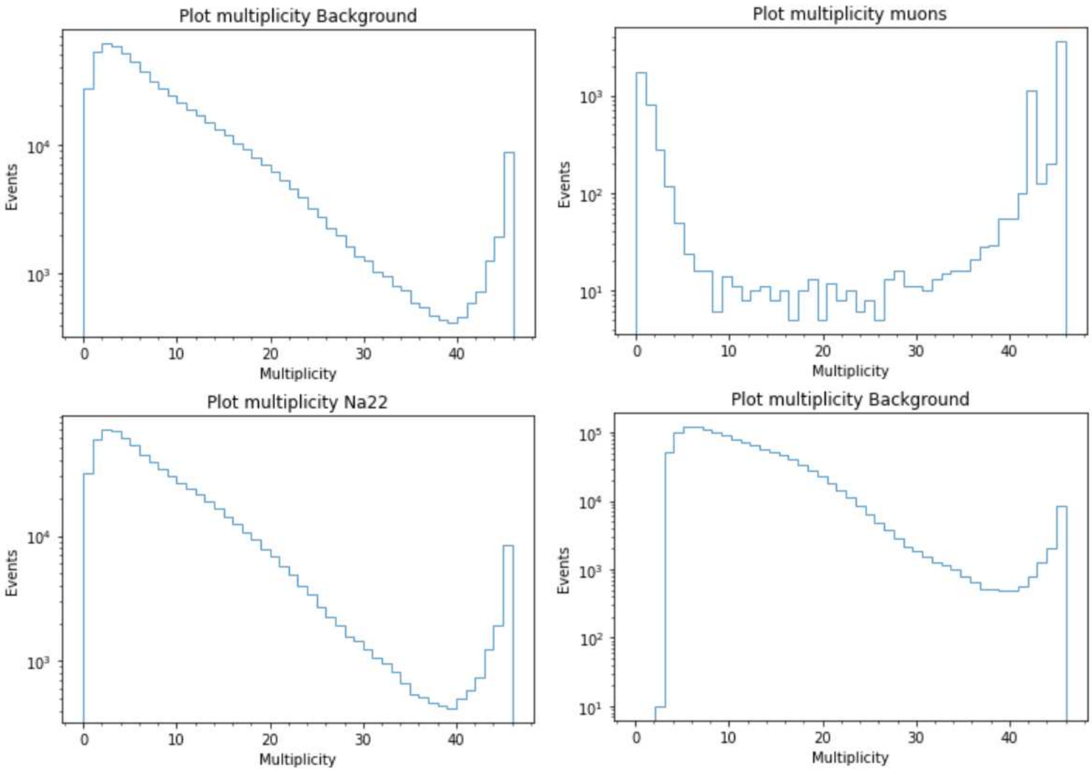

Figure 8: Multiplicity histogram of the four runs

- concerning the cosmic muon multiplicity, a double-peak structure is seen in the plot of figure 8. To understand this structure, a plot of the number of collected events, as a function of the readout channel, is reported in figure 9. It can be noticed that few neighbouring channels have a lower number of events. To further investigate, a plot of the events over their multiplicity is reported in figure 9 and it is possible to notice that for events from a point forward there are no events with $N_{PMT} \geq 42$. This problem is due to some error from the GCUs. Therefore, to select only cosmic muons run that cross almost vertically the acrylic vessel and present no anomaly, a cut of $N_{PMT} \geq 45$ has been applied.

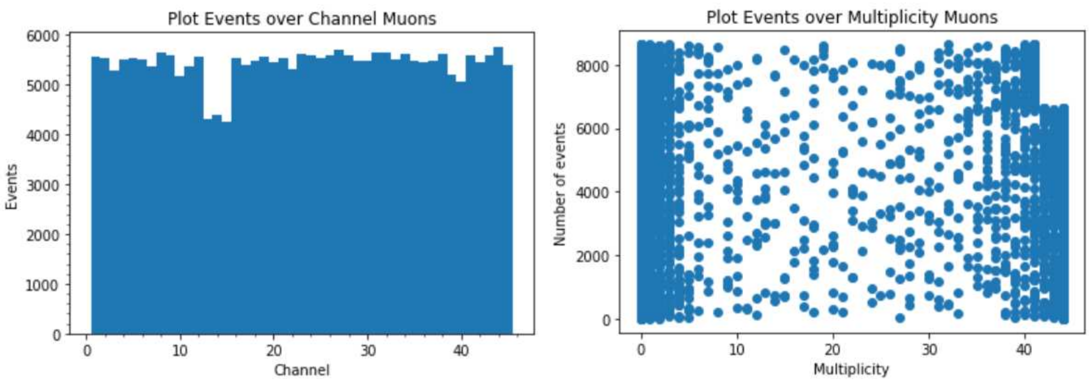

Figure 9: Histogram of the number of events for PMT and graph of the event number over multiplicity

- the timestamp of the events is given in figure 10 and report no anomaly.

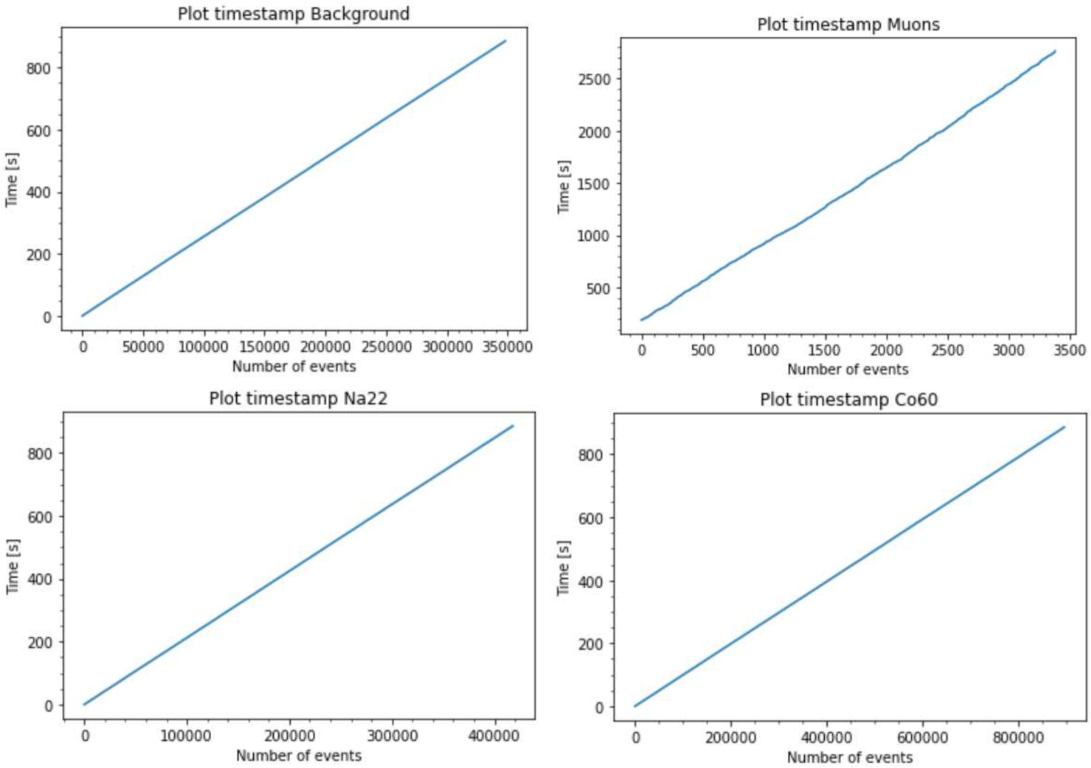

Figure 10: Graph of the timestamp over the number of events of the four runs

- to get an estimate of the rate of the events, the plots of figure 11 give a distribution of the time between two consecutive events. The distribution are fitted with a single exponential function ($A \cdot e^{-b\Delta t}$). The coefficient b of the fit gives an estimate of the events rate during the run. The results are summarized in table 2.

Source	A	b [Hz]
^{60}Co	52475 ± 174	1000 ± 5
^{22}Na	19250 ± 36	471.0 ± 1.3
background	13385 ± 27	391.5 ± 1.2
muons	128 ± 2	1.29 ± 0.03

Table 2: Fit results for the four runs

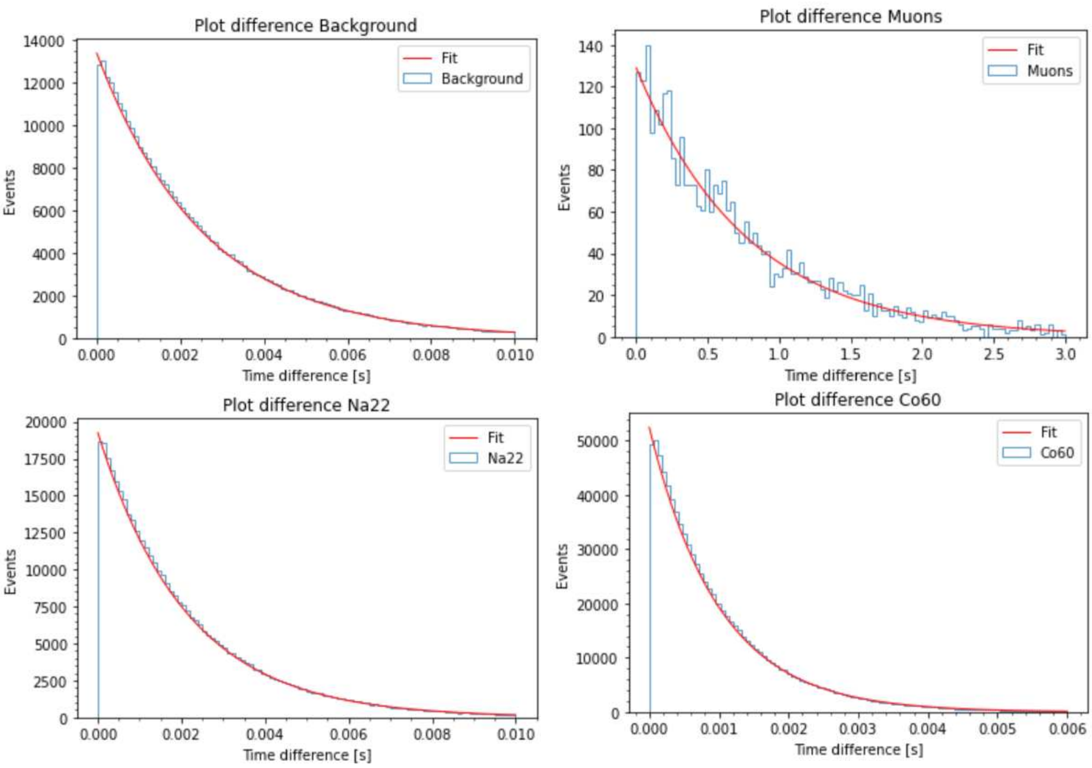

Figure 11: Histogram of the temporal difference between consecutive events with relative fit of the four runs

5 Data analysis

5.1 Charge reconstruction

All the data presented here have all the analysis cuts applied. Now it is possible to generate the histogram of the events for the charge collected by all the PMTs. To do so it is necessary for all waveforms to calculate the integral as $integral = \Delta t_s \cdot \sum_{i=1}^{n} |N_i - B|$ where B is the baseline value (in ADC), N_i is the value of the waveform at the i-th bin and $\Delta t_s = 1ns$. Then from this it is easy to obtain the charge for a PMT as $Q = \frac{integral \cdot 75\mu V}{R}$ with $R = 50\Omega$ which is the expected impedance seen by the PMTs and $1ADC = 75\mu V$ the conversion necessary. To obtain the total charge it is only necessary to sum over all the PMTs.

The total charge reconstruction for the 2 radioactive sources is shown in figure 12 where there is the signal with the background included, only the background and the filtered source spectrum, calculated as the difference between the two histograms.

The charge spectrum for the muons is shown in figure 12 and replicate the expected qualitatively form for energy loss of muons in a liquid scintillator.

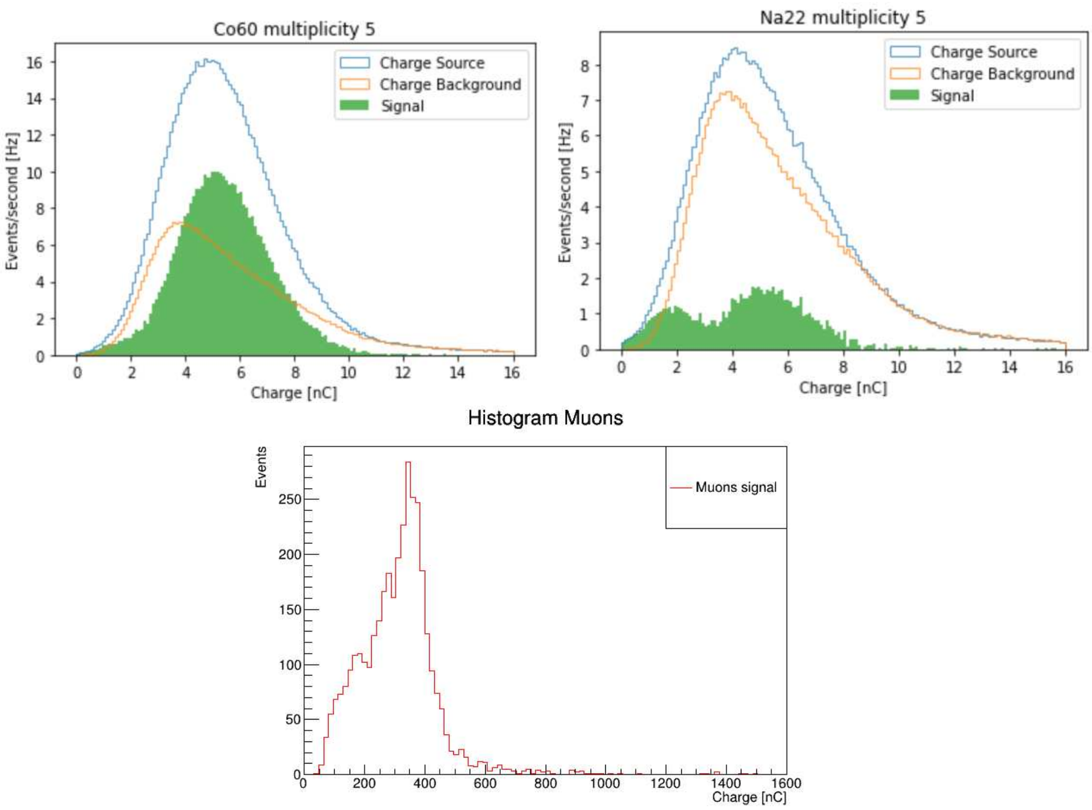

Figure 12: On the left it is reported the ^{60}Co spectrum, on the right the ^{22}Na and on the bottom the muons'

5.2 Muons

Studying the charge spectrum of the muons run it is possible to extract some parameters. In particular it is necessary to use the Crystal Ball function [4][7], defined as

$$CrystalBall(x; N, n, \alpha, \mu, \sigma) = N \cdot \begin{Bmatrix} e^{-\frac{(x-\mu)^2}{2\sigma^2}}, & \frac{x-\mu}{\sigma} > -\alpha \\ A\left(\frac{n}{|\alpha|} - |\alpha| - \frac{x-\mu}{\sigma}\right)^{-n}, & \frac{x-\mu}{\sigma} \leq -\alpha \end{Bmatrix} \textbf{with } A = (\frac{n}{|\alpha|})^n e^{-\frac{|\alpha|^2}{2}} \quad (1)$$

which is a continuous function modeled based on the assumption that for data less than $-\alpha$ it works as a power law of order $-n$ and for data over $-\alpha$ as a Gaussian function with the defined parameter μ, mean value, and σ, the standard deviation. It is also necessary to impose the conditions $\alpha > 0$ and $n > 1$, where both are shape parameters. The N value is a necessary normalization parameter defined such that $CrystalBall(\mu; N, n, \alpha, \mu, \sigma) = N$. Consequentially μ is the charge value that return the highest value of the function, or it can be called the Most Probale Value (MPV).

This function is the theoretical probability distribution for the energy of scintillation photons produced by the interaction of a muon with a liquid scintillator. In particular with the filters applied in the section "Energy calibration Runs" it has been considered only muons that cross the three muons trigger scintillators and the LS vessel, so muons with a vertical direction. In the following image is reported the fit executed with the *CrystalBall* function and the zoomed sector showing which data have been taken in consideration.

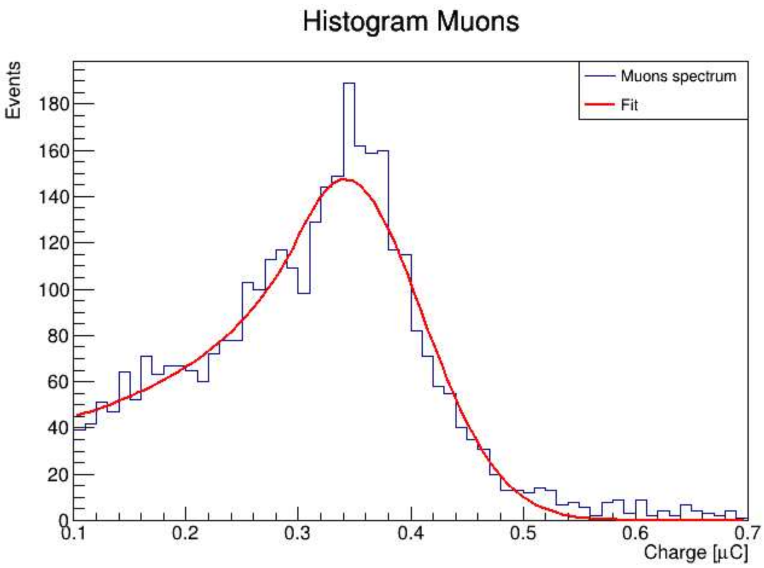

Figure 13: Histogram of the muons spectrum with the *CrystalBall* fit

The resulting fit values and errors are:

$$N = 152 \pm 46 \quad (2)$$

$$n = 1.13 \pm 0.05 \quad (3)$$

$$\alpha = 0.57 \pm 0.05 \quad (4)$$

$$\mu = 0.342 \pm 0.004 [\mu C] \quad (5)$$

$$\sigma = 0.069 \pm 0.003 [\mu C] \quad (6)$$

With a run composed of only events generated by muons it is necessary to have a energy reference, like for the radioactive sources in section "Radioactive sources", to do a energy calibration. In this case it has been used a Monte Carlo simulation that was performed considering cosmic muons at sea level and only with vertical direction (that is why it was important to select only certain events otherwise the Monte Carlo model would have been much more complicated). The basic assumption is that the primary source of muons is the cosmic ray interaction with the atmosphere.

Next with the energy spectrum has been executed a fit calculation with the Landau function in energy defined as:

$$L(x;\mu,\sigma) = \frac{1}{\pi\sigma}\int_0^\infty e^{-t}\cos\left(t\frac{x-\mu}{\sigma} + \frac{2t}{\pi}\log(t\sigma)\right)dt \tag{7}$$

were E is the energy of the event, μ is the Most Probable Value (MPV), which correspond to the same name parameter of the $CrystalBall$ function but measured in MeV, and σ is a width parameter of the probability distribution. The fit returns a value of $\mu = 59 \pm 3[MeV]$ [4].

5.3 Radioactive sources

First of all it is possible to observe that for the previous figures 12 there is no photo peak in the ^{60}Co and ^{22}Na histograms, as expected. Using a LS material we have to use only the Compton spectrum, characterized by the Compton edge, which is the energy for a photon diffused by π degree (phenomena called back scattering). It is also the state which produces a maximum energy for the resulting electron. To understand better the phenomena, the chain reaction is: the gamma photon of the decay is produced, then it enters in the LS and it interacts with an electron, the diffuse electron generates scintillation photons via interaction with the material. The Compton edge value can be calculated with the formula

$$E_{Compton} = E_\gamma\left(1 - \frac{1}{1+\frac{2E_\gamma}{m_e c^2}}\right) \tag{8}$$

where E_γ is the energy of the gamma photon reported previously. For the two radioactive sources we obtain, considering only the $1332KeV$ photon for the ^{60}Co, the table:

Source	$E_{Compton}$ [keV]	E_γ [keV]
^{60}Co	1118	1332
^{22}Na	1062	1275

Table 3: Compton edge values

The model for the rate distribution around the Compton edge value is based on the complementary error function [4] defined as

$$Erfc(x) = \frac{2A}{\sqrt{\pi}}\int_{\frac{x-\mu}{\sigma}}^{+\infty} e^{-t^2}dt + C \tag{9}$$

where the parameter A is the maximum amplitude parameter, C an integral constant and the μ and σ parameter are linked to the Gaussian distribution, which the $erfc$ function is the complementary integral. The fundamental result is μ that represent the Compton edge value and will be used for the calibration fit. The two fit performed with this function are reported in figure 14, in which it has been used only a limited range of data: for the ^{22}Na the range $[4.5 : 12]nC$ and the same for ^{60}Co, both marked by yellow lines in the figure 14. The fit range and binning were chosen to minimize the percentage error of the μ value because it is the only physical parameter necessary. The range limitation choice has been made because for lower charge value the distribution function does not correctly describe the phenomena. This is partially due to the filters applied during the data control and particularly the global trigger validation that remove low multiplicity events, that are also low energy events.

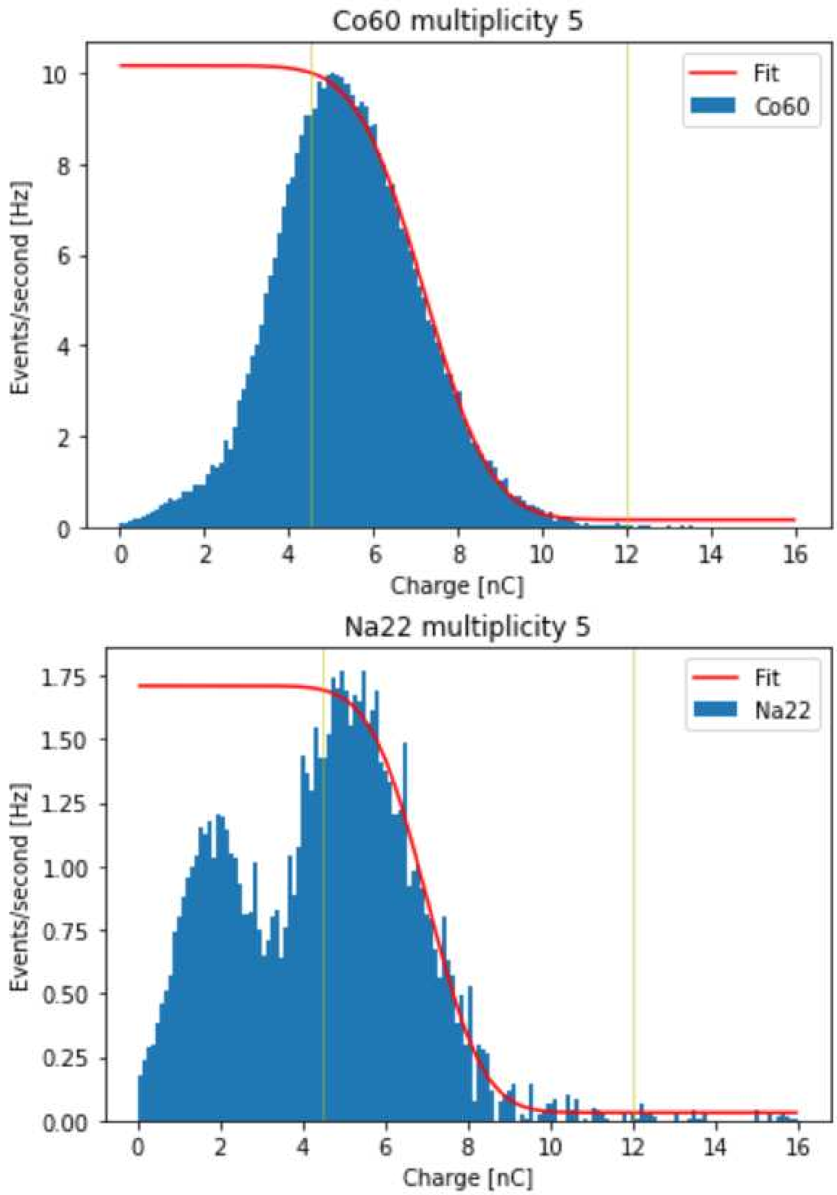

Figure 14: Histogram of the ^{60}Co and ^{22}Na spectrum with the $erfc$ fit

The fit results are:

Source	$E_{Compton}$	$\mu[nC]$	$\sigma[nC]$	$A[Hz]$	C
^{60}Co	1118	7.21 ± 0.03	1.77 ± 0.06	5.00 ± 0.07	0.16 ± 0.05
^{22}Na	1062	7.01 ± 0.06	1.52 ± 0.11	0.84 ± 0.03	0.03 ± 0.02

Table 4: Fit parameters

5.4 Calibration

Now to conclude it is possible to perform a linear regression, with the function $y = ax + b$, and with the data reported in following table calculated in the previous sections:

Source	$E_{expected}[MeV]$	$E_{measured}[nC]$
Muons	59 ± 3	342 ± 4
^{60}Co	1.118	7.21 ± 0.03
^{22}Na	1.062	7.01 ± 0.06

Table 5: Calibration data with the in charge measured value and the energy expected value

The result is shown in figure 15

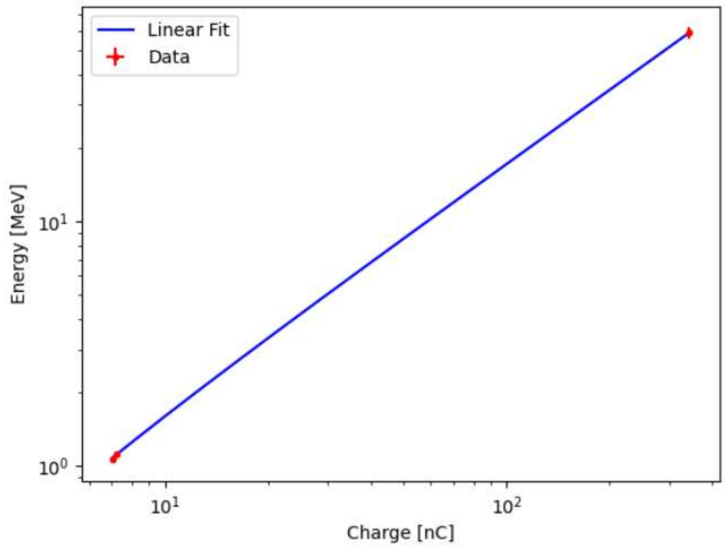

Figure 15: Linear fit graph

and the resulting parameters are

$$a = 0.173 \pm 0.014[\frac{MeV}{nC}] \quad (10)$$

$$b = -0.14 \pm 0.11[MeV] \quad (11)$$

where the parameter a return the conversion value from the charge collected of the event to the energy in MeV.

6 Conclusion

The achieved purpose of the thesis was to study the energy response of the setup mini-JUNO to cosmic muons and to gamma sources, so to conduct an energy calibration. Beginning with a description of the apparatus and the key components used to measure scintillation light four data runs were performed: one background run without any sources, one cosmic muons run, one ^{60}Co run, and one ^{22}Na run.

After the data collection, preliminary data control was conducted, which identified and resolved some problems. Only events meeting specific conditions were selected to contribute to the charge histogram spectrum of the runs. Using these histograms, three parameters (μ) were extracted through fitting with the expected probability distribution functions, and these parameters were used to perform a linear calibration regression.

A crucial future study that can be conducted is a comprehensive examination of the system response, particularly a detailed analysis of the data control section, which could provide valuable insights.

7 Bibliography

References

[1] A. Abusleme et al., “JUNO Physics and Detector”, Progr. Part. Nucl. Phys.123 (2022) 103927, arXiv: 2104.02565

[2] A. Abusleme et al., “JUNO Collaboration”, Chin. Phys. C46 (2022) 123001

[3] V. Cerrone et al., "Validation and integration tests of the JUNO 20-inch PMT readout electronics", Nucl. Inst. Meth. A 1053 (2023) 168322, arXiv: 2212.08454

[4] Riccardo Callegari, ”Characterization and tests of 39 channels of the JUNO large PMT electronics”, Master thesis in physics, Università degli Studi di Padova, (2020).

[5] R. Brun and F. Rademakers, "ROOT An Object-Oriented Data Analysis Framework", Nucl. Inst. Meth. A 389 (19997)81

[6] Recommended data of the Laboratoire National Henri Becquerel: http://www.nucleide.org/DDEP WG/DDEPdata.html

[7] ROOT reference for Crystal Ball function: https://root.cern/doc/master/CrystalBall 8C source.html